THE ASTROPHYSICAL JOURNAL, 547:531–544, 2001 February 1

PRIMORDIAL FRACTAL DENSITY PERTURBATIONS AND STRUCTURE FORMATION IN THE UNIVERSE: ONE-DIMENSIONAL COLLISIONLESS SHEET MODEL

TAKAYUKI TATEKAWA[1] AND KEI-ICHI MAEDA[1,2]

Received 2000 March 9; accepted 2000 September 28

ABSTRACT

The two-point correlation function of galaxy distribution shows that structure in the present universe is scale-free up to a certain scale (at least several tens of Mpc), which suggests that a fractal structure may exist. If small primordial density fluctuations have a fractal structure, the present fractal-like nonlinear structure below the horizon scale could be naturally explained. We analyze the time evolution of fractal density perturbations in an Einstein–de Sitter universe, and study how the perturbation evolves and what kind of nonlinear structure will result. We assume a one-dimensional collisionless sheet model with initial Cantor-type fractal perturbations. The nonlinear structure seems to approach some attractor with a unique fractal dimension, which is independent of the fractal dimensions of initial perturbations. A discrete self-similarity in the phase space is also found when the universal nonlinear fractal structure is reached.

Subject headings: cosmology: theory — large-scale structure of universe

1. INTRODUCTION

The present universe shows a variety of structures. Galaxies are not distributed randomly in the universe. Totsuji & Kihara (1969) and Peebles (1974) showed that the observed two-point correlation function $\xi(r)$ is given by a power law with respect to distance r as $\xi(r) \sim r^{-\gamma}$, with $\gamma \sim 1.8$. Recent galaxy surveys also agree with this result, i.e., the power γ is nearly equal to 1.8; see, e.g., the Center for Astrophysics (CfA; Geller & Hachra 1989), Las Campanas Redshift Survey (LCRS; Jing, Mo, & Börner 1998), and ESO Slice Project (ESP; Guzzo et al. 1998, 2000). This may imply that the present distribution of galaxies is fractal. Sylos Labini, Montuori, & Pietronero (1998) have also claimed that all available data are consistent with a fractal structure with dimension $D \sim 2$ up to the deepest observed scale (1000 h^{-1} Mpc). However, observation of the cosmic microwave background radiation (CMBR) has revealed that the universe in the recombination era is homogeneous and isotropic at least at very large scales. Although CMBR observation seems to be more reliable, we should not decide yet whether or not the large-scale structure of the universe is really fractal up to the horizon scale. To answer this question more definitely, we should await forthcoming galaxy survey projects (Colless 2000; Maddox 1997; Loveday & Pier 1998; Knapp et al. 1999).

However, since it seems true that the galaxy distribution is really fractal up to a certain scale, one might ask how such a structure is formed in the evolution of the universe. One of the most plausible explanations is that the nonlinear dynamics of the perturbations will provide such a scale-free structure during the evolution of the universe. The pioneering work to explain the power-law behavior in the nonlinear stage was done by Davis & Peebles (1977). They assumed a self-similar evolution of density fluctuations and some additional condition, i.e., that a physical velocity $\dot{r}$ vanishes in the nonlinear regime. Then they showed a relation between the power index γ of the two-point correlation function and that of the initial power spectrum n, as $\gamma = 3(n + 3)/(n + 5)$. If we have $n = 0$, then we find that $\gamma = 1.8$. Since their additional condition is not trivial and might not be appropriate, Padmanabhan (1996) and Yano & Gouda (1998a) extended their model to the case with nonvanishing $\dot{r}$. They found that the relation between n and γ is $\gamma = [3h(n + 3)]/[2 + h(n + 3)]$, where $h \equiv -a\langle\dot{x}\rangle/\dot{a}x$, which is the ratio of peculiar velocity to the Hubble expansion. With this result, γ can vary from 0 to 2 for $n = 1$ (Harrison-Zeldovich spectrum) and $0 \leq h \leq 1$ (where $h = 1$ corresponds to the Davis-Peebles solution). Since we do not know the stability of those solutions, in order to find out which value of γ is most likely, we should study the dynamics of density fluctuations using other methods, e.g., N-body simulations. Several groups in fact have showed that a power-law behavior in two-point correlation functions can be obtained by N-body simulations with appropriate primordial density fluctuations (Miyoshi & Kihara 1975; Efstathiou 1979; Aarseth, Gott, & Turner 1979; Frenk, White, & Davis 1983; Davis et al. 1985; Jing 1998).

The question is whether those power-law behaviors mean that we have a fractal structure in the present universe. Peebles (1985) and Couchman & Peebles (1998) showed how to proceed with a high-resolution analysis in the N-body simulation using a kind of renormalization method. They have used the Davis-Peebles solution as a scaling relation. Without such an *Ansatz*, we do not know whether the usual N-body simulation is suitable to discussing the formation of a fractal structure. With the present state of computers, it may not be possible to obtain high enough resolution to analyze a fractal structure.

Another question arises regarding a fractal structure in the universe. Did the universe not have any nontrivial structure, such as fractal, in the initial density fluctuations? In the conventional approaches, initial density perturbations are usually assumed to be given by a power-law (or a power-law–like) spectrum with random Gaussian phase. Although such initial conditions may provide the currently observed nonlinear scale-free structure via nonlinear dynamics, no one has shown whether such a structure is fractal or not, and if so, what kind of fractal structure arises.

[1] Department of Physics, Waseda University, 3-4-1 Okubo, Shinjuku, Tokyo 169-8555, Japan; tatekawa@gravity.phys.waseda.ac.jp, maeda@gravity.phys.waseda.ac.jp.

[2] Advanced Research Institute for Science and Engineering, Waseda University, Shinjuku, Tokyo 169-8555, Japan.

To provide a fractal structure in the present universe, we can adopt an alternative scenario, in which primordial density fluctuations already have a fractal-like structure in the beginning. Note that the background spacetime is assumed to be a smooth Einstein–de Sitter universe, but not a fractal universe. The properties of an initial fractal may be preserved during the evolution of the universe; then nonlinear fractal structure will be formed. In fact, De Gouveia dal Pino et al. (1995) reported that the temperature fluctuation of the CMBR has a fractal relation, and recently Pando & Fang (1998) and Feng & Fang (2000) also reported that non-Gaussianity was detected in the distribution of Lyα forest lines in QSO absorption spectra. In this scenario, several natural questions arise. How does such a primordial fractal perturbation evolve into the nonlinear regime? Will any properties of the initial fractal be preserved during the evolution of the universe, or not? If not, what kind of nonlinear structure will emerge at present? Is there any fundamental difference in the structure formation process between a conventional density perturbation and the present fractal one? In order to answer those questions, we study the time evolution of initial density fluctuations with a fractal structure in an Einstein–de Sitter universe.

Since we are interested in a fractal structure, a quite high resolution is required in our calculation. As we discussed, N-body simulations may not have enough resolution in the present state of computer development, unless we develop some skillful method. Thus, in this paper, we consider only a very simple toy model, which is a one-dimensional sheet model, in order to get some insight into the questions raised above. To set up primordial fractal density perturbations, we distribute N sheets initially by some systematic rule, i.e., we apply a Cantor set or a random Cantor-type set (see below). Mathematically, in order to construct a Cantor set, the procedure must be repeated an infinite number of times, but it is not practically possible to set up such initial data. We therefore stop the procedure at a certain point, i.e., the initial set is given by removing line segments with a given ratio (Falconer 1990) several times. This can be justified because an infinite scale-free structure never exists in the real universe. In order to construct the initial density perturbations, we set that the remaining segments have small positive density perturbations, while the removed segments correspond to small negative ones. Since we study a one-dimensional sheet model, the motion of each sheet is described by an analytic solution (Zeldovich 1970), which guarantees enough resolution to analyze a fractal structure.

In § 2, we present our formalism and initial setting. As for the initial data, we consider three cases: a regular Cantor set, a random Cantor-type set, and random white noise. Comparing those time evolutions, we show our results in § 3. In § 4, we focus particularly on the phase space. The conclusion and discussion follow in § 5.

2. FORMALISM AND INITIAL DATA

2.1. *Dynamical Equations*

In order to study the structure formation of the expanding universe, there are so far three approaches: N-body simulations, the Eulerian perturbation approach, and the Lagrangian one. Although the final answer on structure formation may be obtained by N-body simulations, this approach may not be feasible for answering questions concerning fractal structure. As for the perturbation approaches, these are just an approximation and will break down in the nonlinear regime, although the Lagrangian approach would be better if we are interested in the density perturbations. This is just because the density fluctuation δ and peculiar velocity $\boldsymbol{v}$ are perturbed quantities in the Eulerian approach (Peebles 1980), while the displacement of particles is assumed to be small in the Lagrangian approach (Zeldovich 1970; Bouchet 1992, 1995; Coles & Lucchin 1995; Catelan 1995). Its first-order solution is the so-called Zeldovich approximation (Zeldovich 1970). The Lagrangian approach has been confirmed to be better than the Eulerian approach by comparison of these results in several cases (Munshi, Sahni, & Starobinsky 1994; Sahni & Shandarin 1996; Yoshisato, Matsubara, & Morikawa 1998).

The perturbation variable $\boldsymbol{S}$ in the Lagrangian approach describes a displacement of dust particles from a uniform distribution, and is defined as

$$\boldsymbol{x} = \boldsymbol{q} + \boldsymbol{S}(q, t) , \tag{1}$$

where $\boldsymbol{x}$ and $\boldsymbol{q}$ are the Eulerian and Lagrangian comoving coordinates, respectively. The density fluctuation is given by the Jacobian, J, as

$$\delta(\boldsymbol{q}, t) = \frac{1 - J}{J} , \tag{2}$$

where $J \equiv \det(\partial \boldsymbol{x}/\partial \boldsymbol{q})$.

Even though the Lagrangian approach is better, it is still an approximation and thus is not suitable to discussing highly nonlinear structure formation. However, there is one exceptional case. If the distribution is plane-symmetric, the system is one-dimensional, and then the Zeldovich approximation turns out to be an exact solution. Hereafter, we discuss only one-dimensional problems, the Lagrangian perturbation of which is given by

$$x = q + S(q, t) , \tag{3}$$

where x and q are the one-dimensional Eulerian and Lagrangian comoving coordinates, respectively. For the Einstein–de Sitter model, the solution is given by (Gouda & Nakamura 1989; Bouchet et al. 1995)

$$S(q, t) = a(t)S_1(q) + a(t)^{-3/2}S_2(q) , \tag{4}$$

where the scale factor a changes as $a = (t/t_0)^{2/3}$. Then we find the position and velocity of a dust particle at a scale factor $a(t)$ with respect to the Lagrangian coordinate q as

$$x(q, a) = q + a(t)S_1(q) + a(t)^{-3/2}S_2(q) , \tag{5}$$

$$\tilde{v}(q, a) = S_1(q) - \tfrac{3}{2}a(t)^{-5/2}S_2(q) , \tag{6}$$

where we have introduced a new peculiar velocity, $\tilde{v} \equiv \partial x/\partial a$. In the following discussion, we use the scale factor $a(t)$ as a time coordinate instead of the physical time t.

Although the Zeldovich solution is exact, in studying the formation of nonlinear structure a serious problem will soon arise. As a density fluctuation grows, we find a shell crossing. For a realistic matter fluid, pressure may prevent such a singularity from forming. Then the solution will no longer describe the evolution of perturbations after a shell crossing. However, we may have another choice. If instead of a usual matter fluid we have a collisionless particle, such as some dark matter, we can go beyond the shell crossing. The particles, which are described by plane-parallel sheets, will pass through each other without collision. Then, after this crossing, we rediscover that the Zeldovich solution is

again exact. Therefore, we have a series of exact solutions, which is almost analytic (Gouda & Nakamura 1989; Yano & Gouda 1998b). We call this the one-dimensional sheet model.

To be more precise, when a crossing by two sheets has occurred, those two sheets exchange their numbering as follows. Suppose there are two sheets, q_1 and q_2 ($q_1 < q_2$), with the Eulerian coordinates $x(q_1, a)$, $x(q_2, a)$ [$x(q_1, a) < x(q_2, a)$] and with velocities $\tilde{v}(q_1, a)$ and $\tilde{v}(q_2, a)$, respectively. Assume that these sheets cross over at $a_{\rm cross}$, i.e., $x(q_1, a_{\rm cross}) = x(q_2, a_{\rm cross})$ with $\tilde{v}(q_1, a_{\rm cross}) > \tilde{v}(q_2, a_{\rm cross})$. For the evolution after a shell crossing ($a > a_{\rm cross}$), exchanging their numbering (q_1 q_2) as

$$x(q_1, a_{\rm cross}) \rightarrow x(q_2, a_{\rm cross}) , \quad \tilde{v}(q_1, a_{\rm cross}) \rightarrow \tilde{v}(q_2, a_{\rm cross}) ,$$

$$x(q_2, a_{\rm cross}) \rightarrow x(q_1, a_{\rm cross}) , \quad \tilde{v}(q_2, a_{\rm cross}) \rightarrow \tilde{v}(q_1, a_{\rm cross}) , \quad (7)$$

we again find a natural ordering between the Lagrangian and Eulerian coordinates, i.e., $x(q_1, a) < x(q_2, a)$ for $q_1 < q_2$. By this exchange, we obtain a new distribution of sheets [$x(q, a)$, $\tilde{v}(q, a)$] just after a shell crossing. Using this distribution as initial data, we find a next exact time evolution of the system by the Zeldovich solution. In order to fix the initial data, we must determine $S_1(q)$ and $S_2(q)$ in equation (4) for the given distribution [$x(q, a)$, $\tilde{v}(q, a)$]. From equations (5) and (6) we find that the solution is

$$S_1(q) = \frac{3}{5a}(x - q) + \frac{2}{5}\tilde{v} ,$$

$$S_2(q) = \frac{2}{5} a^{3/2}[(x - q) - a\tilde{v}] . \quad (8)$$

The new exact solution of equation (4) with equation (8) is valid until we encounter next shell crossing, where another two sheets will cross over.

We repeat this prescription every time we encounter a shell crossing. As a result, we obtain a series of Zeldovich exact solutions, which is regarded as an analytic solution for the one-dimensional collisionless sheet model. Note that this prescription is still valid in a multistream region. Using this prescription, Gouda & Nakamura (1989) investigated a time evolution for the density perturbations with a scale-free initial power spectrum. They showed that the power spectrum will approach some characteristic value independent of the power index of the initial spectrum. This characteristic power index -1 is predicted by catastrophe theory. Recently, Yano & Gouda (1998b) investigated the time evolution of the density perturbations for an initial power spectrum with a cutoff. In this case, they found that a self-similarity in all scales is no longer valid. The spectrum is classified into five ranges by its power index. Some spectra coincide with the above one for some scale ranges, but another power index, which is independent of the initial power spectrum, appears just beyond the cutoff scale. In § 5 we show our result compared with their result.

Since this one-dimensional sheet model is powerful enough to see the fine structure, we use this model to analyze the time evolution of the primordial fractal density perturbations.

2.2. *Setting Up Initial Data*

Since we are interested in initial density fluctuations with a fractal distribution, we must construct such initial data. For the sake of simplicity, we apply a Cantor set, or a random Cantor-type set (see below), in our construction. A Cantor set is given by the following procedure. We first divide a line with length L by some integer n_D, and then remove one line segment at the center. If n_D is an even integer, not dividing a line by n_D, we just remove a line segment with the length L/n_D from the center of the line. We then repeat this procedure for the remaining line segments. In the pure mathematical model, the removal procedure must be repeated infinite times. However, we believe that a fractal structure, even if it exists in the universe, is not a mathematical one, but that its self-similarity may end at some scale. Thus, we stop our procedure after a finite number of repetitions. We regard the remaining line segment as a region of positive density fluctuations (δ_+ region), while the removed part corresponds to a region of negative density fluctuations (δ_- region). Here $\delta_+ (> 0)$ and $\delta_- (< 0)$ are chosen to be uniform, i.e., both δ_+ and δ_- are some constants in all regions such that $\delta_+ \simeq |\delta_-| \simeq 10^{-3}$. Although this is very artificial and the realistic perturbations may depend on each scale just like conventional density perturbations, we analyze only this simplest case here (see § 5). In addition to the Cantor set, in order to see the universality of our results we also consider a random Cantor-type set as well as a distribution constructed by white noise. We now describe in more detail how to construct the initial data for each case.

2.2.1. *Regular Cantor Set*

In this case, we consider seven initial data. Each data set is constructed by removing central line segments with a fixed ratio ($1/n_D$, where $n_D = 3$, 6, 8, 10, 12, 15, and 20) from the remaining parts. Each density fluctuation has a different fractal dimension, given by

$$D_0 = \frac{\log 2}{\log [2n_D/(n_D - 1)]} . \quad (9)$$

We assume that $\delta_+ \sim |\delta_-|$. With this *Ansatz*, we have fixed the repetition number of the removal procedure (N_R). Although the number N_R can be different for each initial data set, in order to keep the same resolution for each model (i.e., for the ratio of the smallest line segment l to that of the whole region L [our calculation space] to be almost same), we set $N_R = 5 \sim 7$. We also fix $\delta_+ = 10^{-3}$, which determines the negative density perturbation δ_- such that the mean of fluctuations must vanish (see Table 1).

We show one example of initial data for $n_D = 10$ in Figure 1. We put 2^{17} sheets in our calculation space L. By

TABLE 1

DIVISION PARAMETERS

n_D	D_0	N_R	l/L	δ_-
3.....	0.631	5	1/243	-0.152×10^{-3}
6.....	0.792	6	1/191.10	-0.504×10^{-3}
8.....	0.838	7	1/325.95	-0.647×10^{-3}
10.....	0.868	7	1/267.62	-0.917×10^{-3}
12.....	0.888	7	1/235.36	-1.19×10^{-3}
15.....	0.909	7	1/207.47	-1.61×10^{-3}
20.....	0.931	7	1/183.29	-2.31×10^{-3}

NOTE.—The number of the division n_D, its fractal dimension D_0, the repetition number of removal procedure N_R, the resolution (the ratio of the length of the shortest line segment to that of the whole system l/L), and each negative density perturbation δ_-.

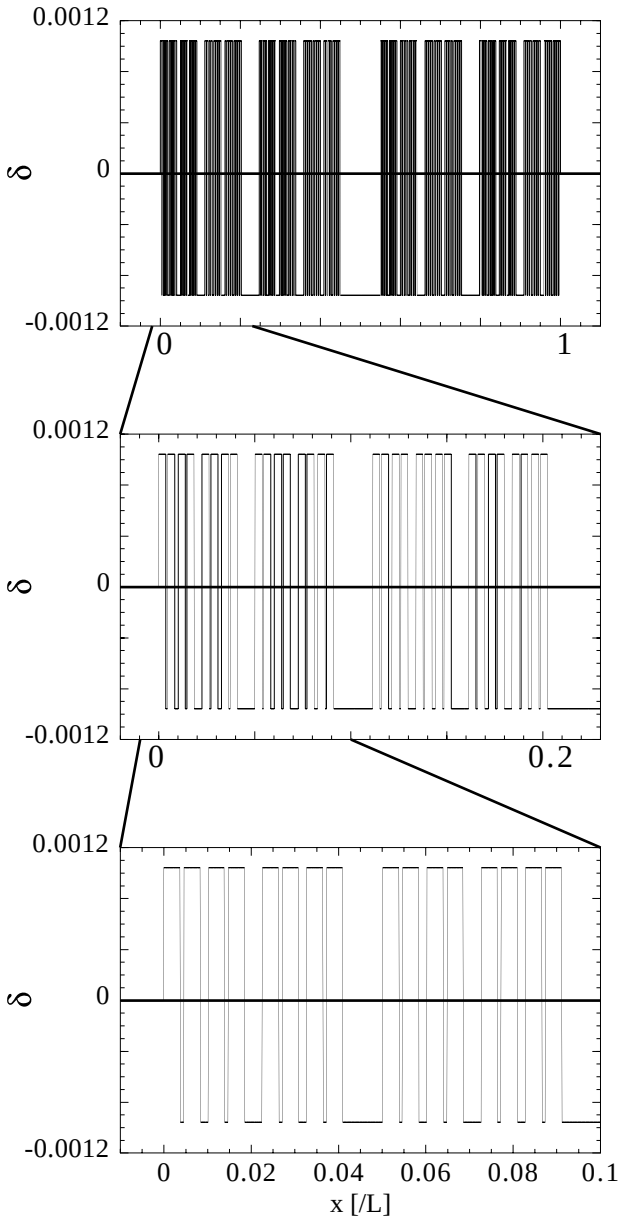

FIG. 1.—Initial fractal density fluctuation for the regular Cantor set with $n_D = 10$. Enlarging the picture, we find the same pattern up to the repetition number of the removal procedure $N_R = 7$.

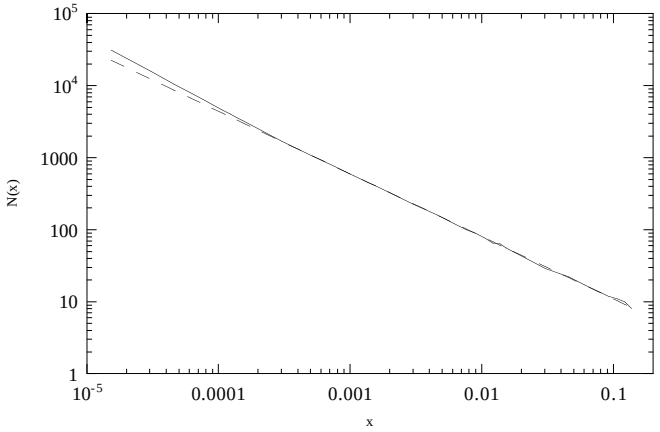

FIG. 2.—Size-number [x-$N(x)$] relation in a box-counting method for the model in Fig. 1. The dotted line shows $N(x) \propto x^{-0.868}$. We find that the similarity exists in the range between $10^{-3}L$ and $10^{-1}L$. Below $x = 10^{-3}L$, we have a deviation from the power-law relation, which corresponds to our resolution limit ($l/L \sim 1/267.62$).

using a box-counting method [the box length x is chosen from $2^{-16}L(\sim 1.5 \times 10^{-5}L)$ to $10^{-1}L$], we have checked the fractal dimension of the initial fluctuations. We calculate the number $N(x)$ of boxes with a length x in which δ_+ segments exist. The result is shown in Figure 2. We find a power law in the x-$N(x)$ relation for the range of $10^{-3}L \le x \le 10^{-1}L$. From this curve, we estimate the fractal dimension as 0.868, which is the same value as that of the present Cantor set. Below $x = 10^{-3}L$, we have a small deviation from a power-law relation, which corresponds to the limit of the resolution of our present model.

Since the Cantor set is quite systematically constructed, one may wonder whether our results strongly depend on such a special setting and so may not be universal. To answer such a question, we also analyze two different initial data settings: one is a random Cantor-type set and the other is just a white noise.

2.2.2. *Random Cantor-Type Set*

The random Cantor-type set is defined such that the division number n_D is fixed as that of a regular Cantor set, while the removal positions of line segments are determined by a random number. According to the box-counting method, we find that the fractal dimension of the initial fluctuations

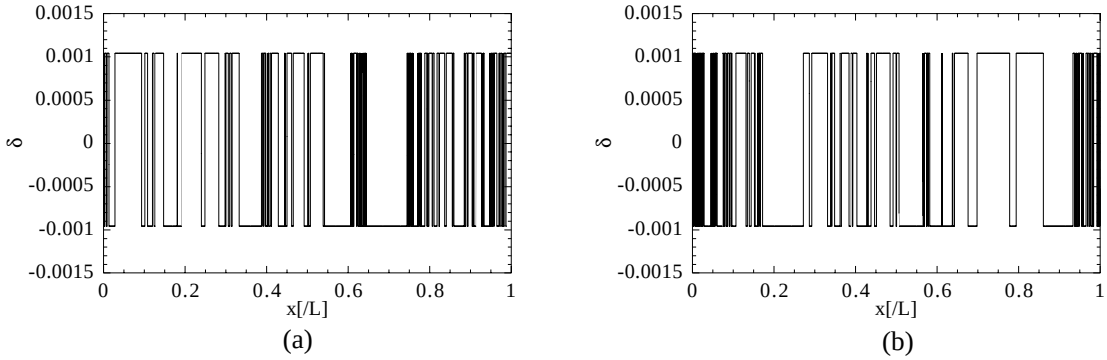

FIG. 3.—(*a*) Initial fractal density fluctuation for the random Cantor-type set with $n_D = 10$. The random Cantor-type set is defined such that the division number n_D is fixed as that of a regular Cantor set, while its removal positions of line segments are determined by a random number. This is called model 1 in the text. Enlarging the picture, we find a similar pattern up to the repetition number of the removal procedure $N_R = 7$. The fractal dimension of this initial fluctuation is 0.868, which is the same as that of the regular Cantor set with $n_D = 10$. (*b*) Another initial fractal density fluctuation set up by the same prescription as (*a*) (model 2).

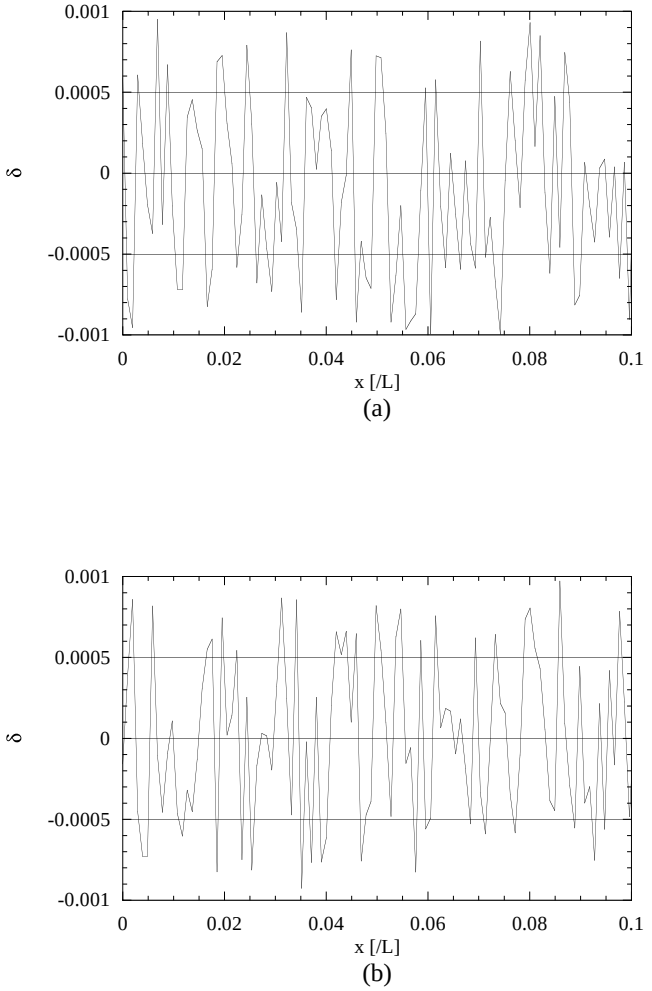

FIG. 4.—(*a*) Initial density fluctuation created by white noise (model 1 in the text). (*b*) Another initial density fluctuation set up by the same prescription as (*a*) (model 2).

is almost the same as that of a regular Cantor set for the same n_D. In this paper, we analyze three random Cantor-type set models: two models with $n_D = 10$ and one with $n_D = 12$. One initial distribution for $n_D = 10$ is shown in Figure 3.

2.2.3. *White Noise*

In order to see whether or not our primordial fractal fluctuations play an important role in structure formation, in particular the formation of fractal structure in the nonlinear regime, we also study the time evolution of primordial fluctuations with white noise. The distribution of initial density fluctuations is given by a random number in the range $-10^{-3} \leq \delta \leq 10^{-3}$. We analyze two models; the initial data for one is shown in Figure 4.

3. TIME EVOLUTION OF PRIMORDIAL FRACTAL DENSITY PERTURBATIONS

In order to see how structures are formed, we must describe the distribution by the Eulerian coordinate. It is convenient to compare the distribution at each time using the comoving coordinate x. We set the initial scale factor $a_0 = 1$. Since our initial density fluctuation is $\sim 10^{-3}$, we find a first shell crossing at $a = a_{\rm cross} \simeq 10^3$. We perform our calculation until $a = (2 \sim 3) \times 10^4$.

In order to see the detail to resolve a fractal structure, we put 2^{17} sheets in our calculation scale L. Using a box-counting method, i.e., counting the number of boxes that contain the region with density perturbation δ larger than 1, we determine the fractal dimension of the nonlinear structures. The size of the box ranges from $2^{-16}L$ to $10^{-1}L$

We now present our results for the three types of initial data, in order.

3.1. *Regular Cantor Set*

First, we show the results for the regular Cantor set with $n_D = 10$. The time evolution is depicted in Figure 5. Because we set $\delta_+ \simeq |\delta_-| \simeq 10^{-3}$, a nonlinear structure appears at $a \simeq 5 \times 10^2$ (Fig. 5*a*). Before a shell crossing, the pattern of density fluctuations remains similar to that of the initial distributions, although each separation will change through gravitational interaction. We then find a shell crossing at $a = a_{\rm cross} \sim 10^3$ (Fig. 5*b*). After the shell crossing, the trace of the initial Cantor set gradually disappears, because of the exchange of the shells by the crossing (Figs. 5*b*–5*f*). Although many sheets cross each other, the peculiar velocities do not vanish immediately because of collisionless sheets, and then the pattern of nonlinear structure will change continuously. After sufficient evolution of the nonlinear structure, we find a self-similarity in the structure, which seems to be fractal. In fact, enlarging some regions, we find similar density distributions (Fig. 6).

In order to judge whether such a structure is fractal or not, we use a box-counting method, which gives a fractal dimension D_F. Before a shell crossing, we find that the dimension D_F decreases in time from the initial value $D_0 = 0.868$, but the error in the estimation increases with time (Fig. 7*a*). This is because although the pattern of initial density fluctuations remains even in a nonlinear stage before a shell crossing, the change of each separation breaks the initial fractal distribution. Then, the initial fractal distribution seems to disappear.

However, after a shell crossing, the fractal dimension starts to increase again and the error in the estimation becomes much smaller. The fractal structure seems to recover. More surprisingly, the dimension D_F approaches some constant ($D_{\rm asym} \sim 0.9$) after $a \simeq 1.5 \times 10^4$, which is a little bit different from the initial fractal dimension $D_0 = 0.868$ (Fig. 7*b*). In fact, $D_F = 0.889 \pm 0.009$ at $a = 1.5 \times 10^4$, and $D_F = 0.890 \pm 0.002$ at $a = 2 \times 10^4$. Although $D_0 = 0.868$ is out of the error bar of D_F, the difference is very small. However, we will see later that D_F is really independent of the initial fractal dimension D_0, in the case of different initial distributions (see Fig. 10, below).

We also calculate the two-point spatial correlation function of nonlinear structures. If the structure is fractal, we have a relation between a fractal dimension and a power index of the correlation function (Falconer 1990). The correlation function here is evaluated for the nonlinear regions in which the density fluctuation δ becomes larger than 1. At $a = 10^3$, just after a first shell crossing, the correlation function shows a rapid oscillation between positive and negative values because of the periodic pattern of the Cantor set. After a shell crossing, the pattern of the Cantor set disappears, and then such an oscillation also vanishes. After enough time passes, i.e., when the stable fractal structure is found, the correlation function also becomes stable (Fig. 8). The function is positive for the distance of $x \leq 5 \times 10^{-2}L$, beyond which it becomes negative, because a shell crossing

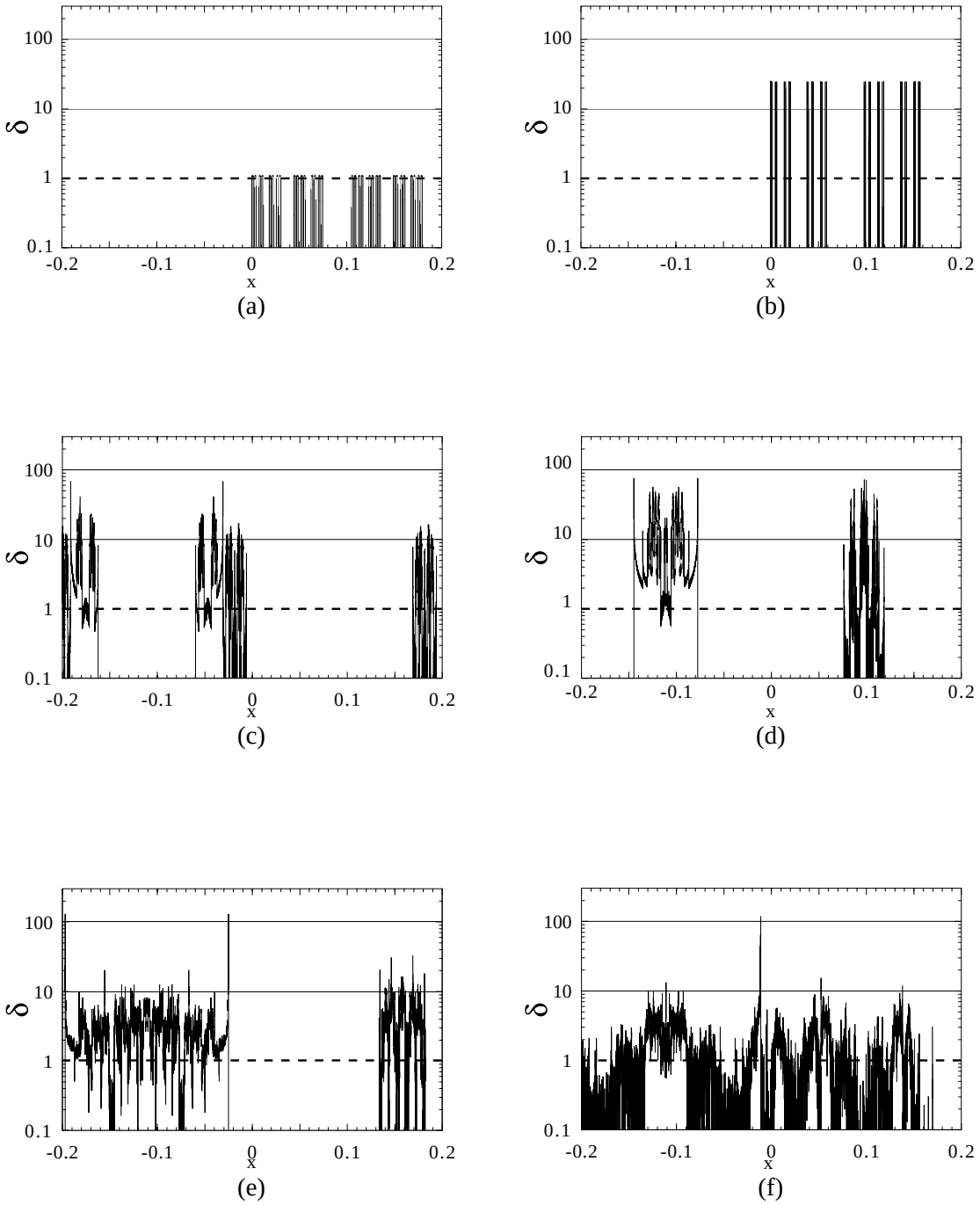

FIG. 5.—Time evolution of density fluctuations for the case with $n_D = 10$; snapshots are at (*a*) $a = 5 \times 10^2$, when the positive fluctuation δ_+ grows just to a nonlinear scale ($\delta_+ = 1$); (*b*) $a \sim a_{\rm cross} \sim 10^3$, which is just after a first shell crossing; (*c*) $a = 6 \times 10^3$; (*d*) $a = 10^4$; (*e*) $a = 1.5 \times 10^4$; and (*f*) $a = 2 \times 10^4$.

does not yet occur for such a scale, and the largest nonlinear structure is about $5 \times 10^{-2} L$. The trace of the initial Cantor set still remains. If the structure is fractal, the correlation function must show a power-law behavior. In fact, from Figure 8, we find a power-law relation in the range of $10^{-4} L < x < 10^{-2} L$ as $\xi \propto x^{-\gamma}$ with $\gamma = 0.130 \pm 0.005$. When the fractal dimension is D_F and the correlation function is given as

$$\xi(x) \propto x^{-(1-D_F)} , \tag{10}$$

then we find $\gamma = 1 - D_F$. The evaluated fractal dimension from the two-point correlation is $D_F = 0.870 \pm 0.005$ at $a = 10000$, which is close to the value obtained by a box-counting $D_F = 0.862 \pm 0.009$. We show the time evolution of two "fractal" dimensions D_F obtained from two-point correlations and by a box-counting method in Figure 9. From Figure 9, we confirm that the power index γ is well correlated with the fractal dimension D_F.

We find a fractal structure after a shell crossing. The fractal dimension is close to the fractal dimension of the initial density distributions. Does this dimension reflect that of the initial distributions? If so, why does it disappear around the first shell-crossing time and recover at a very late time? In order to answer these question, we have looked for other initial conditions with different n_D, i.e., $n_D = 3$, 6, 8, 12, 15, and 20. The fractal dimensions D_0 of the

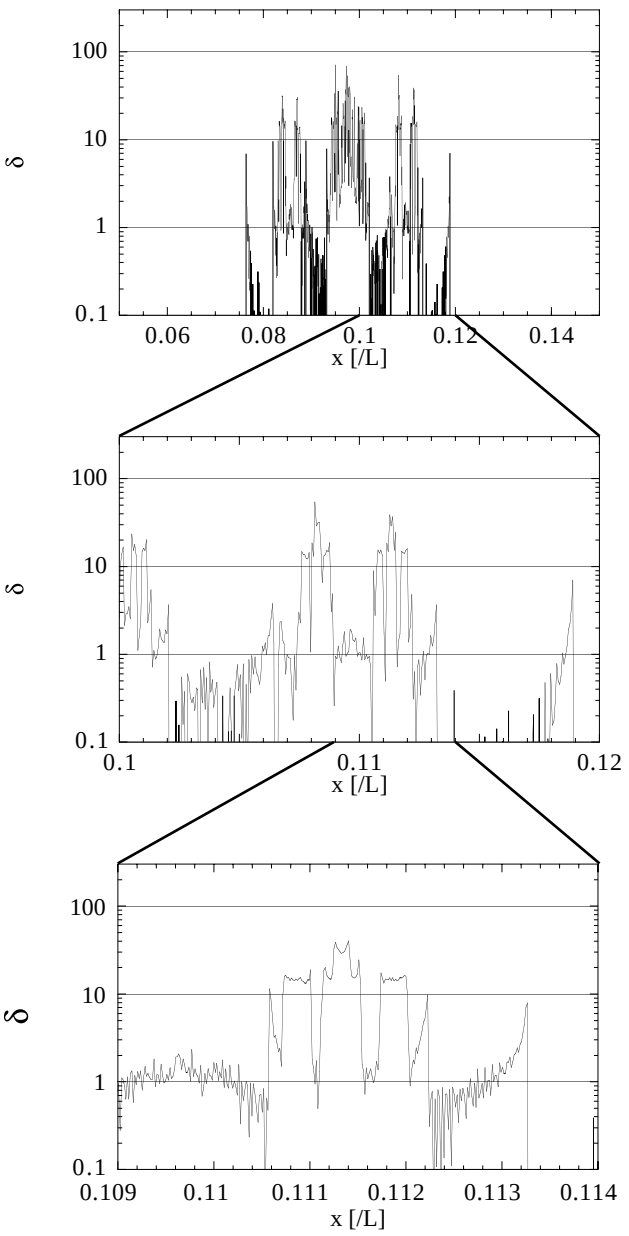

FIG. 6.—Hierarchical nonlinear structure at $a = 10^4$. Enlarging the picture, we find the self-similar structure.

initial density distributions are given in Table 1. As for the time evolution, we find similar behavior for all models. The evolution of the fractal dimension D_F is shown in Figure 10. Surprisingly, for all models, all D_F approach about 0.9 at $a = (2 \sim 3) \times 10^4$, which is the end of our calculation. To confirm our result, we have checked the size-number [x-$N(x)$] relation by a box-counting method, which shows almost a straight line, as in Figure 2. Since the initial dimensions of primordial fluctuations were different, we conclude that the fractal dimension obtained after nonlinear evolution is universal within our numerical accuracy.

3.2. *Random Cantor-Type Set*

Since the Cantor set is highly systematically constructed, one might ask whether the present result strongly depends on such a special initial setting. Is the universal dimension of nonlinear fractal structures due to the primordial density fluctuations defined by the regular Cantor set? In order to answer this question, we analyze a different model with randomness, which we call a random Cantor-type set, defined in § 3.1.

We analyze three models: two models with $n_D = 10$ (model 1 and model 2), and one model with $n_D = 12$. We find that just as in the case of regular Cantor sets, the fractal dimension for nonlinear structures always approaches about 0.9 (Fig. 11). We have also checked the size-number [x-$N(x)$] relation in a box-counting method, finding the same result as in the case of a regular Cantor set. Because we remove a line segment at a random position, we usually expect that the smallest segment will be smaller than that of the regular Cantor set, as we show in the previous subsection. As a result, the stable fractal structure will be formed later than in the case with a regular Cantor set. In fact, in the case of $n_D = 12$, we find the stable dimension (0.9) around $a \simeq 2.3 \times 10^4$ (Fig. 11*c*).

3.3. *White Noise Case*

Another question then arises. Is the universal fractal dimension obtained above via nonlinear dynamics independent of the initial distribution? In order to answer this question, we also analyze a model with white noise fluctuation. We analyze two models. Neither model shows the above universal fractal dimension, although we find some different stable asymptotic dimension ($\sim$0.7; Fig. 12). The error in estimating the dimension is larger than that of the Cantor

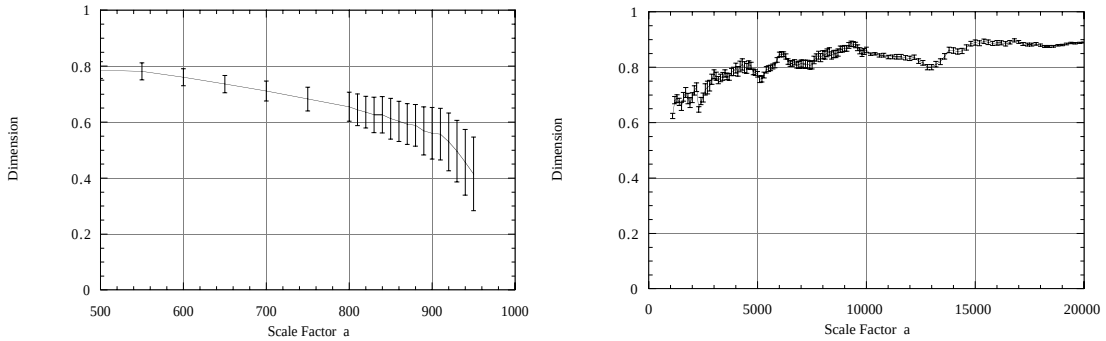

FIG. 7.—Evolution of the fractal dimension D_F of nonlinear structure for the case of $n_D = 10$, (*a*) before a shell crossing ($a < a_{\rm cross} \sim 10^3$) and (*b*) after a shell crossing ($a \geq a_{\rm cross} \sim 10^3$).

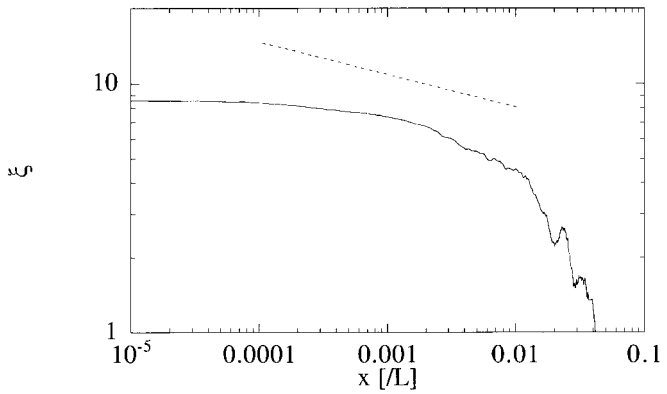

FIG. 8.—Two-point correlation function of nonlinear structures at $a = 10^4$. The dotted line shows $\xi \propto x^{-0.130}$.

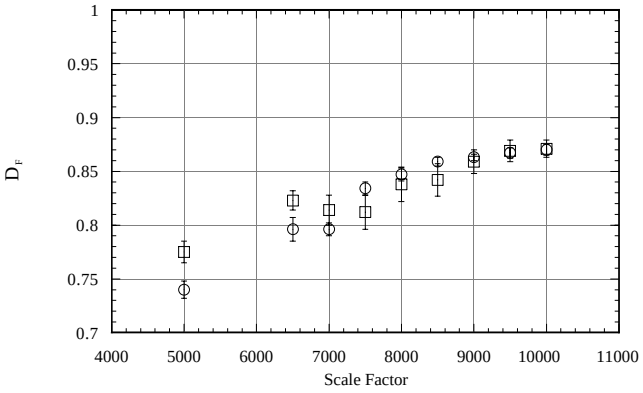

FIG. 9.—Time evolution of the fractal dimensions D_F obtained from the two-point correlation and by a box-counting method. Circles denote D_F from the two-point correlation ($D_F = 1 - \gamma$), while the squares show those produced by a box-counting. The two methods for determining the fractal dimension agree well each other.

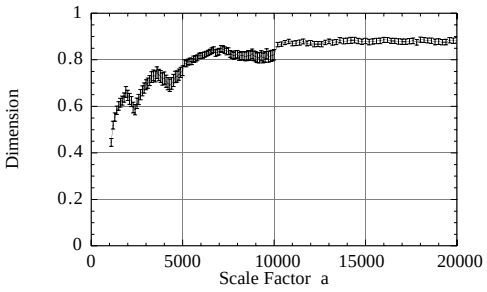

(a)

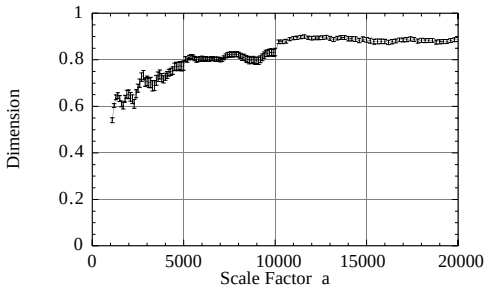

(b)

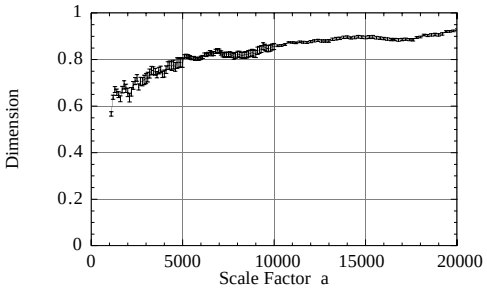

(c)

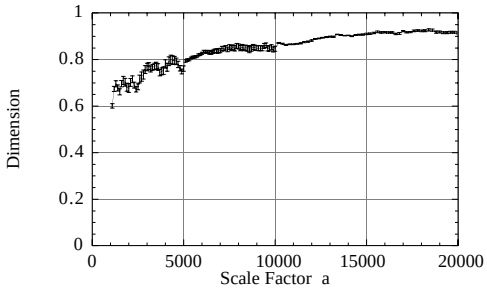

(d)

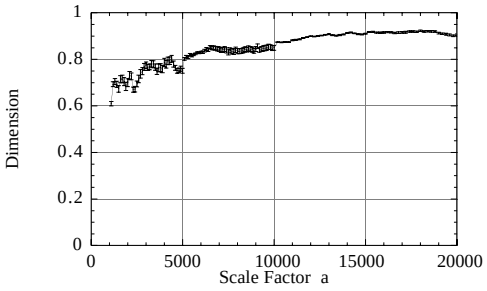

(e)

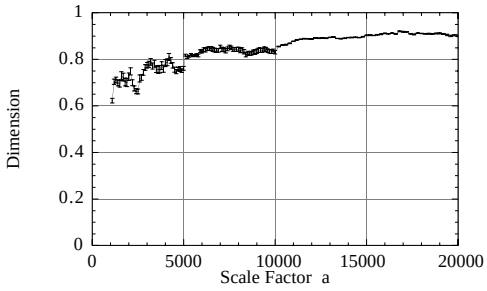

(f)

FIG. 10.—Time evolution of the fractal dimension D_F of nonlinear structure for (*a*) $n_D = 3$, (*b*) $n_D = 6$, (*c*) $n_D = 8$, (*d*) $n_D = 12$, (*e*) $n_D = 15$, and (*f*) $n_D = 20$

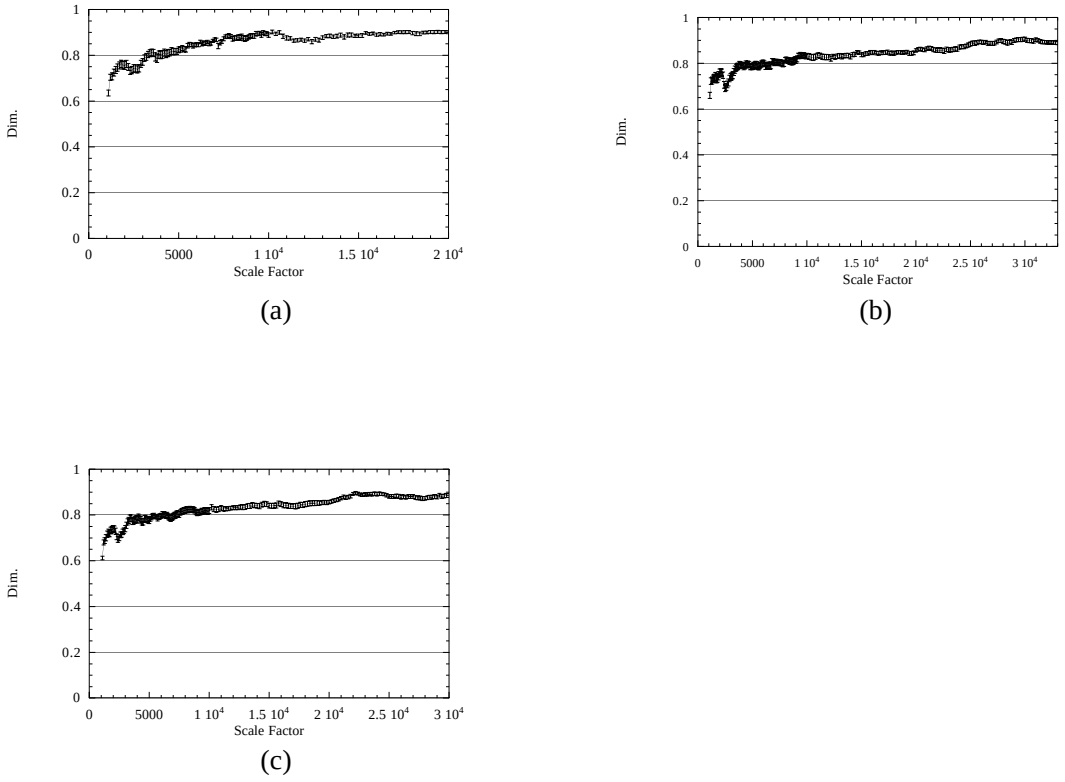

FIG. 11.—Evolution of the fractal dimension D_F of nonlinear structure in the case of the random Cantor-type initial fluctuations for (*a*) $n_D = 10$ (model 1), where the dimension approaches about 0.9 at $a = 2 \times 10^4$; (*b*) $n_D = 10$ (model 2), where the dimension approaches about 0.9 at $a = 2.8 \times 10^4$; and (*c*) $n_D = 12$, where the dimension approaches about 0.9 after $a = 2.3 \times 10^4$.

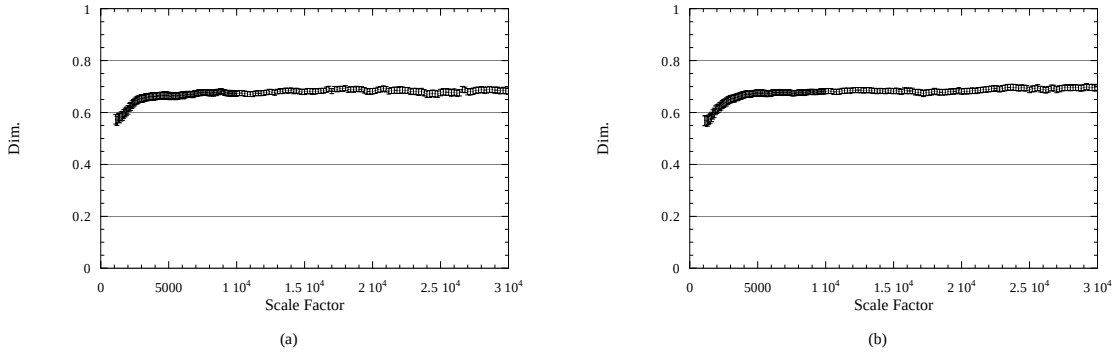

FIG. 12.—(*a*) Evolution of the fractal dimension D_F of nonlinear structure in the case with white noise fluctuations (model 1). The dimension approaches about 0.7. (*b*) Same as (*a*) but for model 2; we also find the same stable dimension 0.7.

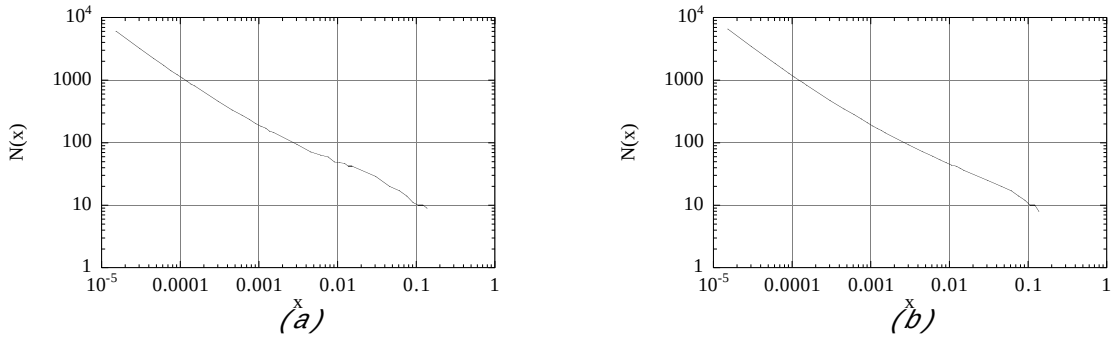

FIG. 13.—Size-number [x-$N(x)$] relations in a box-counting method for the models in Fig. 12. There is some small deviation from a power-law behavior.

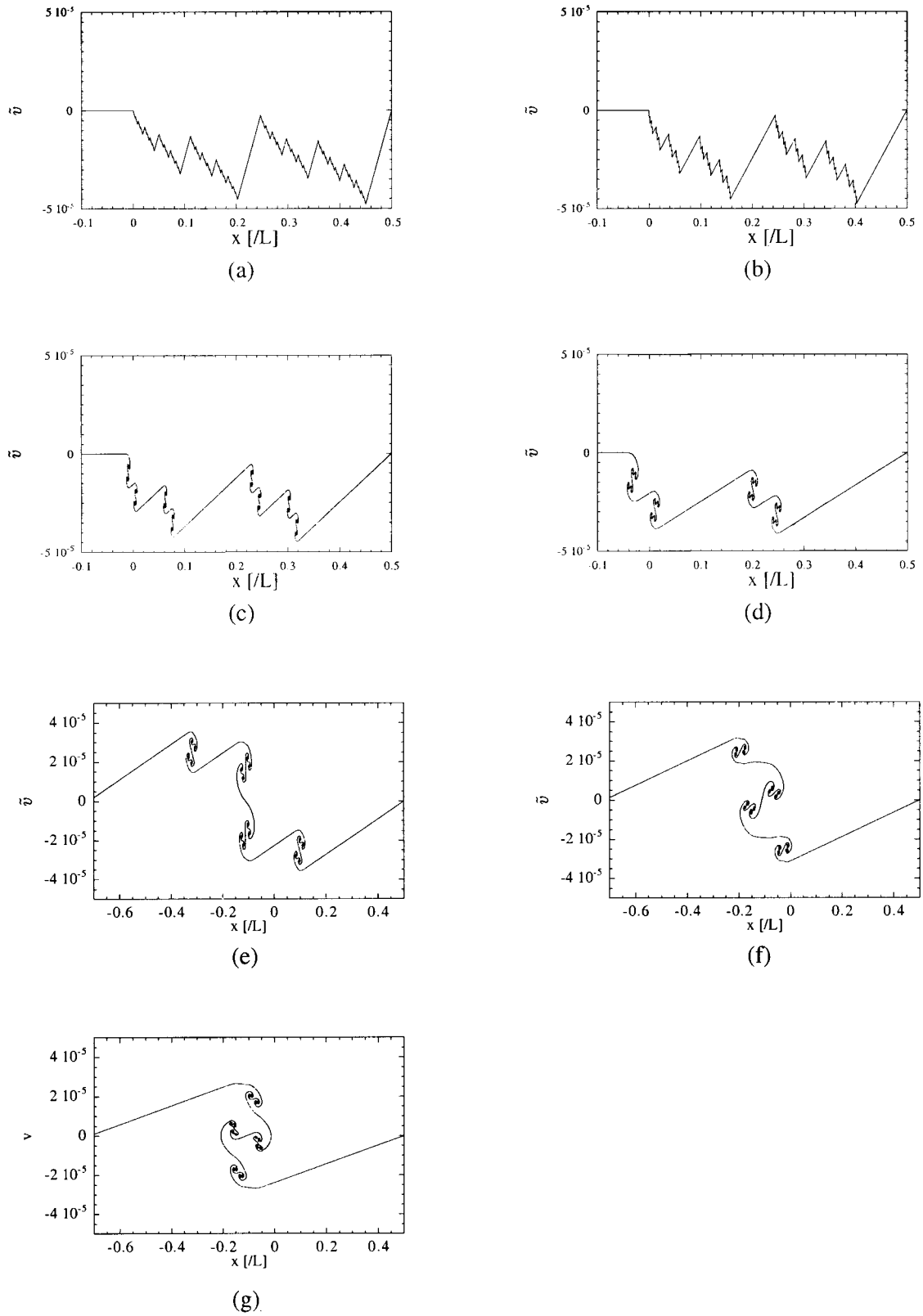

FIG. 14.—Structure formation in the phase space ($n_D = 10$) at (*a*) $a = 1$, where the distribution draws a self-similar graph because the initial density fluctuation is given by a regular Cantor set; (*b*) $a = 10^3$, where immediately after shell crossing, the sheets just begin production of vortices; (*c*) $a = 3 \times 10^3$, where the self-similarity of vortices exists during four steps; (*d*) $a = 5 \times 10^3$, where the self-similarity of vortices exists during five steps; (*e*) $a = 10^4$, where two of the L scale structures begin to combine; (*f*) $a = 1.5 \times 10^4$; and (*g*) $a = 2 \times 10^4$.

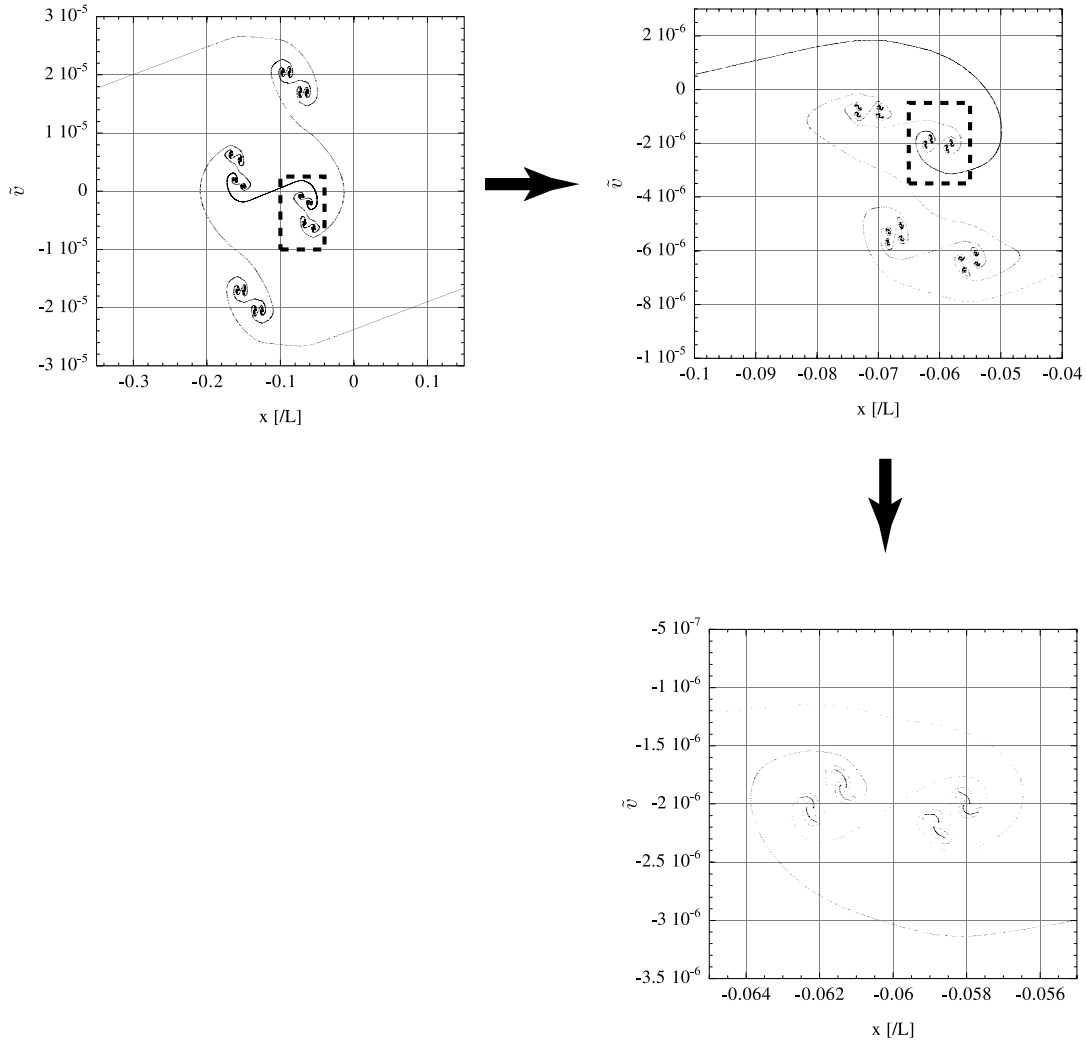

FIG. 15.—Sheet distribution at $a = 2 \times 10^4$ in the phase space ($n_D = 10$). The dotted square regions are enlarged in the next figures, indicated by arrows. We find a discrete self-similarity; i.e., a large vortex consists of some similar small vortices, and those small vortices also consist of similar but much smaller vortices.

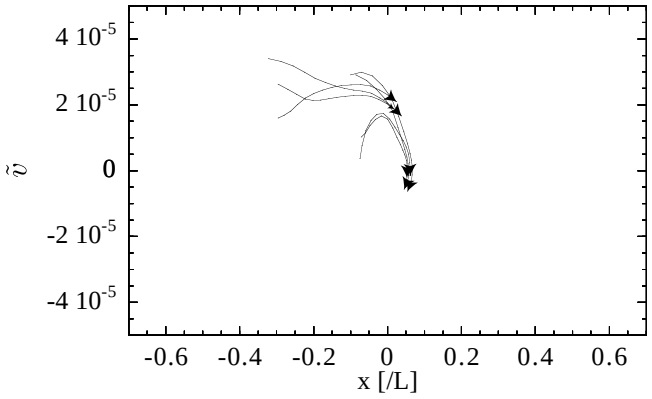

FIG. 16.—Orbits of seven particles in the phase space ($n_D = 10$, $6000 \leq a \leq 20000$). Each particle did not swirl; however, the distribution of particles becomes a set of vortices.

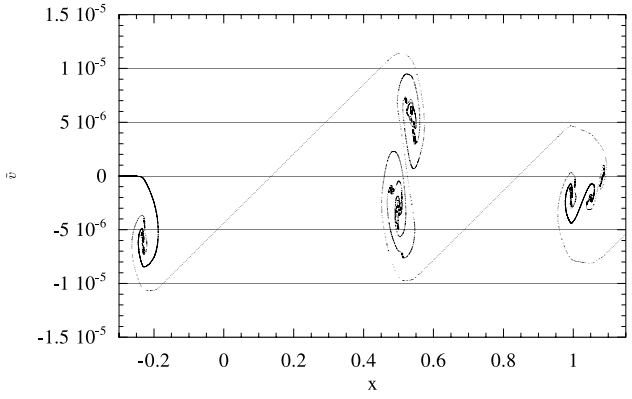

FIG. 17.—Sheet distribution at $a = 30000$ in the phase space for the model with a random Cantor-type set ($n_D = 12$). In this figure, the larger vortices contain smaller vortices, as in the case of the regular Cantor set, but a discrete self-similarity is difficult to find.

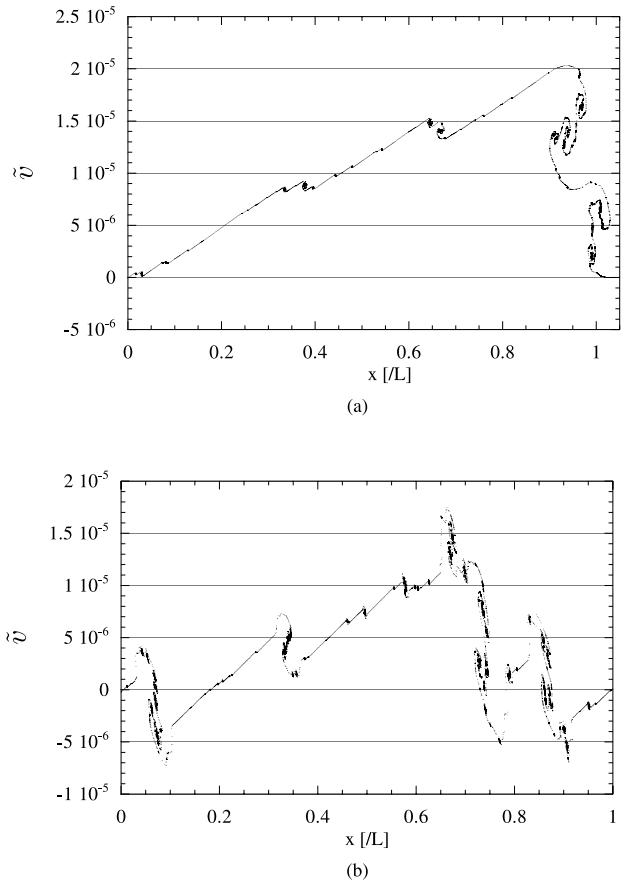

FIG. 18.—Sheet distribution $a = 30{,}000$ in the phase space for the model with white noise fluctuations (model 1). The vortices were widely spread, and a nest of vortices is rarely found.

set model, and the box counting shows some deviation from the power-law relation (Fig. 13). Hence, it would not be a fractal. We discuss this in § 5.

4. PHASE-SPACE ANALYSIS

Although the analysis by box counting suggests that a nonlinear fractal structure with a universal dimension appears from primordial fractal fluctuations, we may get more information from a detailed study of the nonlinear structures obtained. For this purpose, we analyze our result in a phase space.

We show the time evolution of the structures for the regular Cantor set with $n_D = 10$ in the phase space. Initially, the sheet distribution in the phase space is given by a notched curve, because δ_+ and δ_- are constant (Fig. 14). If we enlarge the pictures, we find a similar notched curve due to the present initial setting. These notches reflect a self-similarity in the initial Cantor set. This behavior does not change before a shell crossing (Figs. 14*a* and 14*b*). Only the slopes of the line segments become steeper as a result of the concentration of sheets. After a shell crossing, the curve in the phase space shows very complicated behavior. Two sheets exchanged by a shell crossing are decelerated by mutual gravitational interaction, and then the curve will swirl (Gouda & Nakamura 1989). As the structure evolves, some vortices are combined and form a larger vortex (Fig. 14). When the "fractal" dimension becomes stable around 0.9, we find that the large vortex consists of some similar small vortices. These small vortices also consist of similar but much smaller vortices (Fig. 15). This discrete self-similarity in the phase space is found in all models. As the structure evolves, some vortices are combined and form a larger vortex (Fig. 14). Although the initial fractal distribution seems to disappear, some trace remains in the phase space.

One may wonder why the centers of the vortices appear in the $\tilde{v} > 0$ region (or the $\tilde{v} < 0$ region). The formation of a vortex in the phase space can be easily understood in the case of a single wave ($S_1 = \epsilon \sin q$; see Gouda & Nakamura 1989). In that case, the velocity at the center of the vortex vanishes. Then the appearance of the vortex in the $\tilde{v} > 0$ region (or the $\tilde{v} > 0$ region) seems inconsistent. If we pursue each particle motion, nothing strange happens. They move without swirling except at the $\tilde{v} = 0$ point, as shown in Figure 16.

As was the case with a regular Cantor-type set, we also find similar results in the phase space (Fig. 17). However, a discrete self-similarity is difficult to find, although the larger vortices contain smaller vortices, as in the case of the regular Cantor-type set. In the case with white noise fluctuations, we cannot find any hierarchical vortex structure in the phase space (Fig. 18).

5. CONCLUSIONS AND DISCUSSION

We have studied the nonlinear evolution of primordial fractal fluctuations by using a one-dimensional sheet model. We have analyzed seven models with initial fluctuations constructed by a regular Cantor set, three models with initial fluctuations constructed by a random Cantor-type set, and two models with white noise fluctuations. For all models except the case with white noise, we find a kind of attractor with a universal fractal dimension (~ 0.9) as the fluctuations evolve into the nonlinear regime. In the case with white noise fluctuations, the estimated dimension becomes stable around 0.7, but the error in the estimation is larger than in the other cases, and the power-law behavior in a box-counting method is also not completely fitted. Thus, it may not contain a fractal structure. From the phase-space analysis, we find a hierarchical structure; that is, the large vortex consists of some similar small vortices, and such small vortices again consist of similar but much smaller vortices. In particular, we find a discrete self-similarity for the model with a regular Cantor set.

Why is the fractal dimension close to 0.9? Is it really universal? Is the present fractal structure really an attractor? Although we need more analysis to answer this question, we find some hints in previous work. Gouda & Nakamura studied the present one-dimensional sheet model for the initial power-law spectrum. They found two types of generic singularities when we have a shell crossing (Gouda & Nakamura 1988, 1989). When a first shell crossing appears, the relation between Eulerian and Lagrangian coordinates must be

$$x = q_c + \beta(q - q_c)^3 + \cdots , \tag{11}$$

while the relation after a shell crossing turns out to be

$$x = q_c + \beta(q - q_c)^2 + \cdots . \tag{12}$$

Following Arnold's classification, the former and latter cases are classified into A3 and A2, respectively: A3 is struc-

turally unstable and may appear transiently in the expanding universe, while A2 is structurally stable and appears universally for the initial power-law spectrum. The latter case gives

$$\delta_k = \int \delta(x) e^{ikx}\, dx \propto \int (\beta x)^{-1/2} e^{ikx}\, dx = (\beta k)^{-1/2} \int \eta^{-1/2} e^{i\eta}\, d\eta\,, \tag{13}$$

i.e., $P(k) \sim k^{-1}$. This predicts $\gamma = 0$, i.e., $D_F = 1$, which is rather close to our "universal" dimension 0.9. Although one may wonder whether these are essentially the same, we have another result that suggests that there seems to exist a new type of stable phase. Recently, Yano & Gouda analyzed a more realistic case, i.e., the initial power-law spectrum with a cutoff, and found five characteristic regions in Fourier space (Yano & Gouda 1998a, 1998b). Regime 1 is the linear one, and is just an initial power spectrum. In regime 2, they found $P(k) \sim k^{-1}$, which is the single-caustic regime (Gouda & Nakamura 1989). Regime 3 is called the multicaustic regime, in which the power spectrum depends on the initial power-law index. Beyond the cutoff scale, two regimes appear. The first gives $P(k) \sim k^{-1}$ (regime 5), which may correspond to the A2 type stable solution. In the intermediate wavenumber k between the regime 3 and regime 5, they find k^{ν}, where ν is independent of the initial power index and close to 1, but a little less. They called this the virialized regime. This seems to be a new transient region, which may appear in some specific initial conditions. We would conjecture that the fractal structure with a universal dimension 0.9 corresponds to this virialized regime (regime 4), and the dimension 0.7 found in the case with white noise would be regime 3. By reanalyzing the Yano-Gauda model in the case of $k = 0$, we have confirmed that $\nu = \sim 0.9$. We also find a small tail with index 0.7 in the size-number relation in the Cantor set model with $n_D = 15$ and 20 (Fig. 19).

This conjecture is also supported by analysis for a self-gravitating one-dimensional sheet model without background expansion of the universe (Tsuchiya, Konishi, & Gouda 1994). They found two timescales: the first is a micro relaxation time ($t_{\rm micro} = Nt_c$), while the other is a global relaxation time ($t_{\rm global} = 4 \times 10^4 Nt_c$), where $t_c = (L/4\pi GNm)^{1/2}$ is a crossing time. After $t_{\rm micro}$, some equilibrium state is reached by exchanging particle energy, but the global relaxation is not achieved, i.e., the partition function is not yet described by an equilibrium state such as an ergodic state (Tsuchiya et al. 1994). In the present model, we can speculate that the fractal structure is obtained after this micro relaxation time but before the global relaxation time. In fact, if we estimate the above timescales in the present models, we find that $t_{\rm micro}$ corresponds to $a = 5 \times 10^3$, while $t_{\rm global}$ corresponds to $a = 5 \times 10^6$. The time at which we find a stable fractal structure [$a = (1 \sim 3) \times 10^4$] is between these two timescales. If this speculation is true, our fractal structure is temporal. In the future of the universe, it will evolve into a more relaxed and ergodic state.

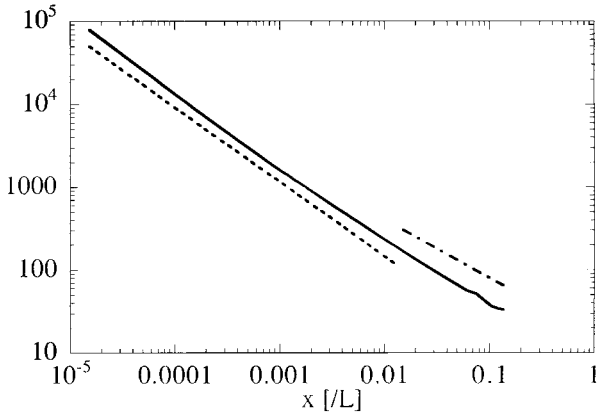

FIG. 19.—Size-number [x-$N(x)$] relation in a box-counting method for the regular Cantor set with $n_D = 15$ at $a = 30{,}000$. The dotted line denotes $N(x) \propto x^{-0.9}$, while the dot-dashed line is $N(x) \propto x^{-0.7}$.

Since we analyze the simplest case, we must extend our analysis to more generic cases. First, we should study different types of fractals in order to check whether the present results are universal for any fractal distributions. Second, we need to analyze the case with scale-dependent fluctuations. In the present analysis, we set $\delta_+ = $ const. and $\delta_- = $ const. In the realistic case, there must be a scale dependence to the fluctuations. In the conventional perturbations, we usually assume a power-law spectrum with some cutoff. Even if the primordial fluctuations contain a fractal structure, their amplitude may depend on the scale. Its dependence may change the present results. In particular, in the present model, the scenario of structure formation could be different from either top-down or bottom-up for some scale dependence. The primordial fractal fluctuations will evolve directly into a hierarchical nonlinear structure. However, it will definitely depend on the scale dependence of the fluctuations. Second, we need to extend the present analysis to other cosmological models, i.e., the open universe model and the $\Lambda \neq 0$ flat universe model. For the one-dimensional sheet model, the solutions are still exact, and the growth and decay rates in these models are different from those in the Einstein–de Sitter universe model. We expect that the structure formation after a shell crossing is not the same as that in the present cosmological model, and then the fractal dimension would be different.

For more realistic cases, we must study either a two- or three-dimensional model. Since the Zeldovich solution is no longer exact, we must explore a new method. In order to preserve a high resolution, we may develop a kind of renormalization method in N-body simulations, as in Couchman & Peebles (1998).

Finally, it would also be interesting to look for the origin of such a primordial fractal density perturbation. The inflationary scenario may provide the origin of primordial fluctuations. One may wonder whether such a fractal primordial fluctuation is expected in some inflationary models. If we have more than two scalar fields, then the system is not integrable and may show a chaotic behavior or a fractal property (Easther & Maeda 1999). Such a model might show some kind of fractal density perturbation.

We would like to thank N. Gouda, P. Haines, O. Iguchi, T. Kurokawa, V. Lukash, M. Morikawa, A. Nakamichi, Y. Sota, T. Yano, and A. Yoshisato for many useful discussions. Part of this work was done while K. M. was participating the program "Structure Formation in the

Universe" at the Newton Institute, University of Cambridge. K. M. is grateful to the Newton Institute for their hospitality. Our numerical computation was carried out by Yukawa Institute Computer Faculty. This work was supported partially by a Grant-in-Aid for Scientific Research Fund of the Ministry of Education, Science and Culture (Specially Promoted Research 08102010), and by the Waseda University Grant for Special Research Projects.

REFERENCES

Aarseth, S. J., Gott, J. R., III, & Turner, E. L. 1979, ApJ, 228, 664
Bouchet, F. R., Colombi, S., Hivon, E., & Juszkiewicz, R. 1995, A&A, 296, 575
Bouchet, F. R., Juszkiewicz, R., Colombi, S., & Pellat, R. 1992, ApJ, 394, L5
Catelan, P. 1995, MNRAS, 276, 115
Coles, P., & Lucchin, F. 1995, Cosmology (New York: John Wiley)
Colless, M. M. 2000, Publ. Astron. Soc. Australia, 17, in press
Couchman, H. M. P., & Peebles, P. J. E. 1998, ApJ, 497, 499
Davis, M., Efstathiou, G., Frenk, C. S., & White, S. D. M. 1985, ApJ, 292, 371
Davis, M., & Peebles, P. J. E. 1977, ApJS, 34, 425
de Gouveia dal Pino, E. M., Hetem, A., Horvath, J. E., de Souza, C. A. W., Villela, T., & de Araujo, J. C. N. 1995, ApJ, 442, L45
Easther, R., & Maeda, K. 1999, Classical Quantum Gravity, 16, 1637
Efstathiou, G. 1979, MNRAS, 187, 117
Falconer, K. 1990, Fractal Geometry (New York: Wiley)
Feng, L., & Fang, L. Z. 2000, ApJ, 535, 519
Frenk, C. S., White, S. D. M., & Davis, M. 1983, ApJ, 271, 417
Geller, M. J., & Huchra, J. P. 1989, Science, 246, 897
Gouda, N., & Nakamura, T. 1988, Prog. Theor. Phys., 79, 765
———. 1989, Prog. Theor. Phys., 81, 633
Guzzo, L., et al. 1998, in Wide Field Surveys in Cosmology, ed. S. Colombi & Y. Mellier (Paris: Editions Frontières), 85
———. 2000, A&A, 355, 1
Jing, Y. P. 1998, ApJ, 503, L9
Jing, Y. P., Mo, H. J., & Börner, G. 1998, ApJ, 494, 1
Knapp, J., Gunn, J., Margon, B., Lupton, R., York, D., & Strauss, M. 1999, The Sloan Digital Sky Survey Project Book, http://www.astro.princeton.edu/PBOOK/welcome.htm
Loveday, J., & Pier, J. 1998, in Wide Field Surveys in Cosmology, ed. S. Colombi & Y. Mellier (Paris: Editions Frontières), 317
Maddox, S., et al. 1998, in Large Scale Structure: Tracks and Traces, ed. V. Mueller et al. (Singapore: World Scientific), 91
Miyoshi, K., & Kihara, T. 1975, PASJ, 27, 333
Munshi, D., Sahni, V., & Starobinsky, A. A. 1994, ApJ, 436, 517
Padmanabhan, T. 1996, MNRAS, 278, L29
Pando, J., & Fang, L. Z. 1998, A&A, 340, 335
Peebles, P. J. E. 1974, A&A, 32, 197
———. 1980, The Large Scale Structure of the Universe (Princeton: Princeton Univ. Press)
———. 1985, ApJ, 297, 350
Sahni, V., & Shandarin, S. 1996, MNRAS, 282, 641
Sylos Labini, F., Montuori, M., & Pietronero, L. 1998, Phys. Rep., 293, 61
Totsuji, H., & Kihara, T. 1969, PASJ, 21, 221
Tsuchiya, T., Konishi, T., & Gouda, N. 1994, Phys. Rev. E, 50, 2607
Yano, T., & Gouda, N. 1998a, ApJ, 495, 533
———. 1998b, ApJS, 118, 267
Yoshisato, A., Matsubara, T., & Morikawa, M. 1998, ApJ, 498, 48
Zeldovich, Ya. B. 1970, A&A, 5, 84